ACS APPLIED MATERIALS & INTERFACES

Research Article

www.acsami.org

# Origin of Enhanced Hole Injection in Organic Light-Emitting Diodes with an Electron-Acceptor Doping Layer: p-Type Doping or Interfacial Diffusion?

Lei Zhang, Feng-Shuo Zu, Ya-Li Deng, Femi Igbari, Zhao-Kui Wang,* and Liang-Sheng Liao*

Jiangsu Key Laboratory for Carbon-Based Functional Materials & Devices, Institute of Functional Nano & Soft Materials (FUNSOM), and Collaborative Innovation Center of Suzhou Nano Science and Technology, Soochow University, Suzhou, Jiangsu 215123, China

Supporting Information

**ABSTRACT:** The electrical doping nature of a strong electron acceptor, 1,4,5,8,9,11-hexaazatriphenylene hexacarbonitrile (HATCN), is investigated by doping it in a typical hole-transport material, *N*,*N*′-bis(naphthalen-1-yl)-*N*,*N*′-diphenylbenzidine (NPB). A better device performance of organic light-emitting diodes (OLEDs) was achieved by doping NPB with HATCN. The improved performance could, in principle, arise from a p-type doping effect in the codeposited thin films. However, physical characteristics evaluations including UV−vis absorption, Fourier transform infrared absorption, and X-ray photoelectron spectroscopy demonstrated that there was no obvious evidence of charge transfer in the NPB:HATCN composite. The performance improvement in NPB:HATCN-based OLEDs is mainly attributed to an interfacial modification effect owing to the diffusion of HATCN small molecules. The interfacial diffusion effect of the HATCN molecules was verified by the in situ ultraviolet photoelectron spectroscopy evaluations.

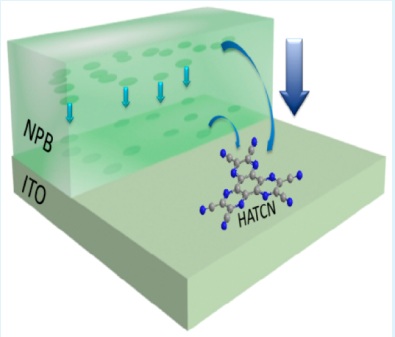


**KEYWORDS:** *organic light-emitting diodes, doping, electron acceptor, charge transfer, carrier injection, interfacial diffusion*

## 1. INTRODUCTION

Improving the device performance of organic light-emitting diodes (OLEDs) has drawn much attention recently because of their remarkable application in flat-panel display and solid-state lighting.[1,2] Lowering the driving voltage is one of most important issues from the viewpoint of low consumption. Because of the low intrinsic carrier concentration of organic semiconductors, optimization of carrier injection from the electrodes to the emitting organic semiconductors is desired with the goal of fabricating low-voltage and highly efficient organic electronic devices.[3−6] Especially for hole injection, there exist large energy barriers between the organic materials and the electrodes because of the large offset of energy levels between the work function of commonly used indium−tin oxide (ITO) and the highest occupied molecular orbital (HOMO) of hole-transporting layers (HTLs).[7,8] Many efforts, such as inserting pristine interlayers and/or electron-acceptor-doped (p-type doping) interlayers, have been carried out to tune the hole injection at the ITO/organic interfaces.[9−13] In particular, some electron-accepting materials, i.e., molybdenum trioxide ($MoO_3$)[14−17] and tetrafluorotetracyanoquinodimethane ($F_4$-TCNQ),[18−21] have been reported as excellent p-type dopants by modifying the energy levels of the anode and the wide-band-gap HTLs. In an acceptable view, the modified energy interface and enhanced carrier injection are attributed to the doping effect in doped organic host materials through electrons transfer from organic molecules to the dopants. Similar to $MoO_3$ and $F_4$-TCNQ, 1,4,5,8,9,11-hexaazatriphenylene hexacarbonitrile (HATCN) was assumed to be a p-type dopant for hole-transport materials because it has six carbonitrile units with strong electron-withdrawing character.[22−29]

In general, p-type doping is achieved by doping strong electron acceptors to an organic host material, with the electron affinity of the dopant molecule in the ionization energy range of the host, that is, charge transfer from the HOMO of the host to the lowest unoccupied molecular orbital (LUMO) of the p-type dopant. Once p-type doping occurs, improved hole injection and lowered driving voltage can be achieved in practical OLEDs. In recent experiments, we found that enhanced hole injection does not simply originate from the effect of p-type doping for all host:dopant systems. An interface doping effect, in which some strong electron acceptors can diffuse out of the doped system by thermal motivation during deposition or field motivation during device operation with a modification effect on the acceptor/metal interfaces, also occurs in some mixed host:dopant systems. In this work, we investigate the injection properties as well as the "doping" behavior of HATCN in a typical hole-injection and -transport material, *N*,*N*′-bis-(naphthalen-1-yl)-*N*,*N*′-diphenylbenzidine (NPB).[30−33] The

Received: March 5, 2015
Accepted: May 13, 2015
Published: May 13, 2015





DOI: 10.1021/acsami.5b01989
ACS Appl. Mater. Interfaces 2015, 7, 11965−11971

experimental results demonstrate that a HATCN-doped NPB interfacial layer showed limited improvement of hole-injection ability in OLEDs. Prior to the occurrence of charge transfer, the enhanced hole injection is mainly attributed to anode modification by HATCN since interdiffusion of HATCN small molecules through the NPB interlayer toward the anode. The measurements of UV−vis absorption spectra, Fourier transform infrared (FTIR) absorption, and X-ray photoelectron spectroscopy (XPS) reveal that there is not efficient charge transfer from the HOMO of NPB to the LUMO of HATCN to form a p-type doping effect. From the in situ ultraviolet photoelectron spectroscopy (UPS) evaluations, it was verified that the HATCN molecules may diffuse through the NPB layer toward the ITO surface (interfacial diffusion effect) and precisely adjust the energy levels at ITO (interface modification effect), which reduces the hole-injection barrier (HIB) for NPB.

## 2. EXPERIMENTAL SECTION

**2.1. Device Fabrication and Characterization.** Materials of $MoO_3$, HATCN, NPB, tris(8-hydroxyquinoline)aluminum ($Alq_3$), 4-(dicyanomethylene)-2-*tert*-butyl-6-(1,1,7,7-tetramethyljulolidyl-9-enyl)-4*H*-pyran (DCJTB), 4,4′,4″-tri-*N*-carbazolyltriphenylamine (TCTA), 4,4′-bis(carbazol-9-yl)biphenyl (CBP), 2′,2″-(1,3,5-benzinetriyl)tris(1-phenyl-1*H*-benzimidazole) (TPBi), bis(2-phenylpyridine)(acetylacetonate)iridium(III) [$Ir(ppy)_2(acac)$], and 8-hydroxyquinolinolatolithium (Liq) were purchased from Lumtec Company and used as received. OLED devices were prepared on ITO (110 nm and 15 Ω/□) glass substrates. The substrates were first cleaned with a detergent solution and solvents and then exposed to UV ozone for 15 min before deposition of the materials. The active area of each device is 0.09 $cm^2$. All of the layers were thermally deposited in a high-vacuum deposition system with a base pressure of ~$10^{-6}$ Torr. Deposition rates and thicknesses of all materials were monitored with oscillating quartz crystals. Codeposition from individual sources with different monitors was used for the doping material system. The deposition rate of NPB was controlled at 0.2 nm/s, and the deposition rate of the guest was adjusted according to the volume ratio doped in the host materials. All devices were encapsulated by cover glasses before the performance test. The electroluminescence and current density−voltage ($J$−$V$) characteristics were measured by a constant-current source (Keithley 2400 sourcemeter) combined with a photometer (Photo Research SpectraScan PR 655).

**2.2. Physical Characterization of Organic Films.** The absorption spectra of NPB, NPB:HATCN (5 vol. %), and NPB:$MoO_3$ (20 vol. %) films were measured with a UV−vis spectrophotometer (PerkinElmer Lambda 750). The transmission IR spectrum was recorded from a FTIR microscope (Bruker VERTX 70). UPS and XPS measurements were carried out in a Kratos AXIS Ultra-DLD ultrahigh-vacuum (UHV) surface analysis system. XPS measurements using a monochromatic Al K$\alpha$ source (1486.6 eV) were conducted to study the charge-transfer conditions with a resolution of 0.4 eV. UPS analysis was performed to characterize the valence states and vacuum level (VL) with an unfiltered He I (21.2 eV) lamp and a total instrumental energy resolution of 100 meV. For UPS measurements, organic thin films were in situ thermally deposited onto UV-ozone-treated ITO substrates in the interconnected deposition chamber. Samples were transferred to the analysis chamber without breaking the vacuum. The Au $4f_{7/2}$ peak position and the Fermi level ($E_F$) edge of a gold film were used to calibrate the binding energy (BE) scale, and all the UPS and XPS spectra are referred to $E_F$ as zero BE.

**2.3. In Situ Interface Evaluation by UPS.** Interface studies were carried out in situ in a Kratos AXIS Ultra-DLD UHV surface analysis system, consisting of a fast load lock (base pressure <1 × $10^{-8}$ Torr), an evaporation chamber (<5 × $10^{-10}$ Torr), a multiport carousel chamber (<5 × $10^{-10}$ Torr), and an analysis chamber (<3 × $10^{-10}$ Torr). Gold films of 600 Å were deposited on precleaned ITO substrates. Organic materials were then in situ thermally deposited onto the gold substrates at room temperature with a growth rate of 1 Å/min at a pressure of 2 × $10^{-9}$ Torr. After each deposition step, samples were transferred to the analysis chamber without breaking the vacuum. UPS measurements were performed to characterize the valence states and VL by using the He I excitation line (21.2 eV) from a helium discharge lamp with a total instrumental energy resolution of 0.1 eV, and samples were negatively biased to enable the observation of secondary electron cutoffs. All of the spectra were obtained at room temperature.

## 3. RESULTS AND DISCUSSION

**3.1. Influence of HATCN Doping on the Device Performance.** It has been confirmed that $MoO_3$ can form a p-type doping effect with many organic materials by accepting charges from organic host molecules.[14−17] The interface doping effect of HATCN really occurs when pristine HATCN is utilized as an interlayer between ITO and NPB HTL.[26,27] After the HTL was doped by HATCN, a lowered driving voltage and improved power efficiency can be achieved, as shown in Figure S1 in the Supporting Information (SI), agreeing with the previous reports.[22,28] However, there are few reports on the p-type doping effect of HATCN and the direct evidence of charge transfer in HATCN-doped hole-transport materials. To find the origin behind this, we first investigate the influence of HATCN doping on the OLED performance by using pristine HATCN and HATCN-doped NPB as a hole-injection layer (HIL). The current density−voltage ($J$−$V$) and power efficiency−current density ($\eta$−$J$) characteristics of ITO/HIL (45 nm)/NPB (30 nm)/$Alq_3$:DCJTB 1 vol. % (20 nm)/$Alq_3$ (10 nm)/$Alq_3$:Li 1 vol. % (30 nm)/Al (100 nm) with pristine HATCN and HATCN-doped NPB as the HILs are shown in parts a and b of Figure 1, respectively. As shown in Figure S2 in the SI, OLEDs with pristine $MoO_3$ and $MoO_3$-doped NPB as the HILs are also

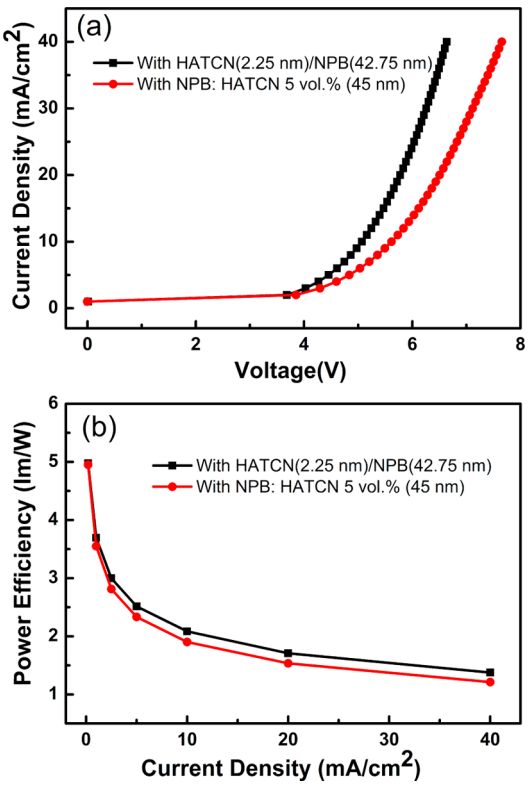


**Figure 1.** (a) $J$−$V$ and (b) $\eta$−$J$ characteristics of devices with pristine HATCN or HATCN-doped NPB as the HILs.


DOI: 10.1021/acsami.5b01989
ACS Appl. Mater. Interfaces 2015, 7, 11965−11971

shown for comparison. The doping ratios of HATCN and $MoO_3$ in NPB are optimized based on the device performance. As reported in the literature,[14,15] lowered driving voltage and improved power efficiency were observed in NPB:$MoO_3$-based OLEDs compared to those using pristine $MoO_3$ as an HIL. However, the device with a HATCN-doped NPB HIL showed an increased driving voltage and a decreased power efficiency compared to those using pristine HATCN as the HIL.

HATCN has strong electron-withdrawing capabilities with its six carbonitrile units. HATCN has also been reported as the electron acceptor when it was doped into some hole-transporting materials.[28,34,35] However, nearly no obvious improvement in the OLED performance was observed when using HATCN-doped NPB as an HIL in OLEDs. What is more, few reports mentioned direct evidence of the formation of charge transfer in HATCN-doped hole-transport materials. Therefore, we suspect the occurrence of charge transfer in NPB:HATCN composite films. A clear image of the "doping" effect in a NPB:HATCN host:dopant system needs to be clarified.

**3.2. Physical Characteristics in HATCN-doped NPB Composite Films.** For the p-type doping effect, charge transfer takes place in two models. One is for integer charge transfer from the HOMO of the host to the LUMO of the p dopant. This mutual ionization is then argued to result in a localized charge on the dopant and a mobile hole in the host. Another is that molecular orbital hybridization forms between the HOMO of the host and the LUMO of the dopant, leading to the formation of a charge-transfer complex.[14−17] UV−vis and FTIR absorption and XPS are very useful techniques for confirming charge transfer in a host:dopant system by getting the structural information at the molecular levels.

Figure 2 shows the UV−vis absorption spectra of the NPB and NPB:HATCN (5 vol. %) films both with a thickness of 45 nm on quartz substrates. The measurement of NPB:$MoO_3$ (20 vol. %) films is also shown for comparison. Different from $F_4$-TCNQ-[35] and $Mo(dft)_3$[37]-doped systems, no additional absorption peaks are observed in the HATCN-doped NPB film. This suggests that charge transfer is suppressed in HATCN-doped NPB films. Comparably, $MoO_3$-doped NPB films demonstrate additional absorption peaks at around 494 and 1380 nm as a result of the formation of CTC, which agrees well with past reports.[38,30]

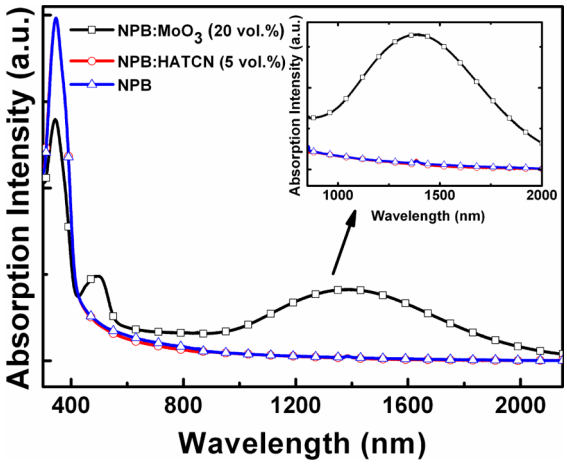


**Figure 2.** UV−vis absorption spectra of the NPB, NPB:HATCN (5 vol. %), and NPB:$MoO_3$ (20 vol. %) films with the same thickness of 45 nm on quartz substrates.

Figure 3 shows the FTIR spectra of the NPB, NPB:HATCN (5 vol. %), NPB:$MoO_3$ (5 vol. %), and NPB:$MoO_3$ (20 vol. %) films. The inset is the calculated HOMO level distribution of NPB. The electrons in the HOMO are mostly located on the nitrogen atom, the terminal and bridging phenyl groups, and part of the naphthyl moieties according to the calculated HOMO distribution. If the electrons in the HOMO of the NPB can transfer to the acceptor molecules, a change of the electronic distribution and vibrational structure will take place, the peaks of which on behalf of the electronic distribution and vibrational structure will become weaker or even lost. This indicates that charge transfer really exists. Transmission modes of the FTIR spectra in the NPB:HATCN (5 vol. %) composite film are found to be almost the same as those in the pristine NPB film, indicating that there is no chrage-transfer complex in the HATCN (5 vol. %)-doped NPB composite films. However, in the cases of NPB:$MoO_3$ (5 vol. %) and NPB:$MoO_3$ (20 vol. %), the peaks around 1592, 1573, 1491, 1392, 1293, and 769 $cm^{-1}$, which correspond to the electronic properties of the phenyl and naphthyl groups, become weaker or almost disappeared compared to the pristine NPB film. As shown in the inset of Figure 3, the HOMO electrons of NPB mainly locate on the phenyl and naphthyl groups. This suggests that charge transfer from the HOMO of NPB to the conduction band of $MoO_3$existed, which results in a change of the electronic distribution and vibrational structure in the phenyl and naphthyl groups of NPB:$MoO_3$ composite films.[39]

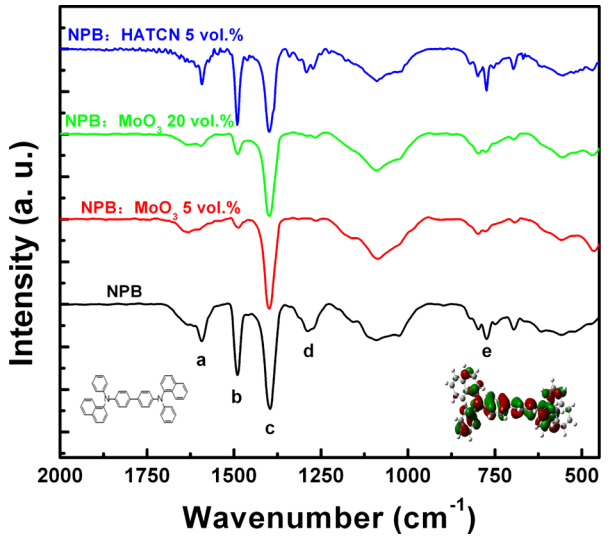


**Figure 3.** FTIR spectra of the NPB, NPB:HATCN (5 vol. %), NPB:$MoO_3$ (5 vol. %), and NPB:$MoO_3$ (20 vol. %) films. Inset: chemical structure and calculated HOMO level distribution of NPB. The band marked a around 1592 and 1573 $cm^{-1}$ is assigned to a CC stretching vibration involving the terminal phenyl groups (*tert*-phenyl) and a naphthyl CC stretching mode. The b band at 1491 $cm^{-1}$ corresponds to a CC/CN stretching and CH bending vibration that is associated with both the terminal and bridging phenyl groups. The c vibration at 1392 $cm^{-1}$ involves CC/CN stretching + CH bending of the naphthyl moieties of NPB. The d band at 1293 $cm^{-1}$ is attributed to a CH/CCN bending + CN stretching vibration involving the terminal and bridging phenyl groups. The e band with a frequency of 769 $cm^{-1}$ is assigned to the out-of-plane CH wag of the naphthyl groups of NPB.


DOI: 10.1021/acsami.5b01989
ACS Appl. Mater. Interfaces 2015, 7, 11965−11971

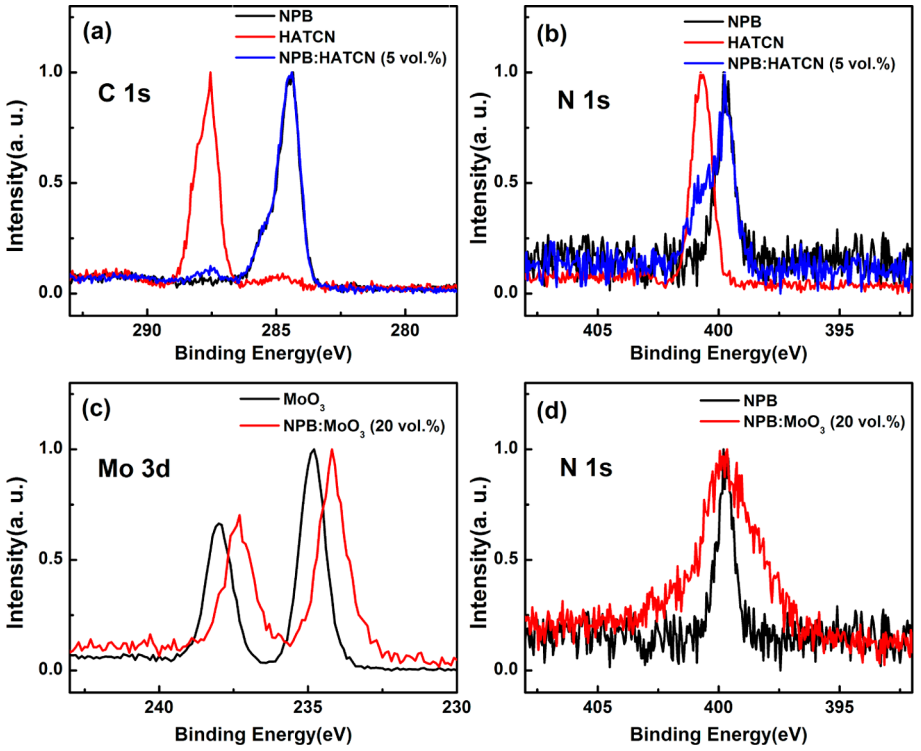


**Figure 4.** XPS core-level spectra of (a) C 1s and (b) N 1s of NPB, HATCN, and NPB:HATCN (5 vol. %) films, (c) Mo 3d of $MoO_3$ and NPB:$MoO_3$ (20 vol. %) films, and (d) N 1s of NPB and NPB:$MoO_3$ (20 vol. %) films.

Figure 4 shows the XPS core-level spectra of (a) C 1s and (b) N 1s of NPB, HATCN, and NPB:HATCN (5 vol. %) films, (c) Mo 3d of $MoO_3$ and NPB:$MoO_3$ (20 vol. %) films, and (d) N 1s of NPB and NPB:$MoO_3$ (20 vol. %) films. No obvious peak shifts or new peaks for C 1s and N 1s were observed in the NPB:HATCN composite films. The C 1s and N 1s spectra of the composite films are just the stacking spectra of the pristine NPB film and the HATCN film. In the case of NPB:$MoO_3$ (20 vol. %) as shown in Figure 4c,d, the Mo 3d peaks shift to lower BE compared to the pristine $MoO_3$ film and the N 1s peak is broadened compared to the pristine NPB film, which suggests that there was partial charge transfer between NPB and $MoO_3$ molecules.[12,40] This means that charge transfer really occurred in $MoO_3$-doped NPB films but not in NPB:HATCN composite films. The UV absorption spectra and XPS results also correspond with the energy levels. The HOMO of NPB is around 5.5 eV,[30−33,41] while the conduction band of $MoO_3$ is around 6 eV,[42−44] which is below the HOMO of NPB. Therefore, electron transfer from the HOMO of NPB to the conduction band of $MoO_3$ is expected, which could explain the UV and XPS results in the case of NPB:$MoO_3$ films. However, the LUMO of HATCN is 5.1 eV,[45] located higher than the HOMO of NPB, and no charge transfer is expected. The *J*−*V* curves of hole-dominated devices in Figure S4 in the SI also indicate no doping effect by charge transfer in the NPB:HATCN film.

**3.3. Interdiffusion of HATCN from a Doped NPB Interlayer.** The device performance and physical evaluation suggest that there was no efficient charge transfer between the NPB host and HATCN dopant. This deduces that the slightly improved performance in NPB:HATCN-based OLEDs was attributed to an interfacial modification of ITO by the interdiffused HATCN molecules from the doped NPB layer. To confirm this assumption, the hole-injection characteristics of different HIL-based devices are investigated. Considering that the total amount of HATCN used inside the NPB:HATCN 5 vol. % (45 nm) film will be about 2.25 nm if we deposit the HATCN film only, the device with HATCN (2.25 nm)/NPB (42.75 nm) interlayers was fabricated for comparison. Their *J*−*V* characteristics in double-logarithmic plots are shown in Figure 5. The *J*−*V* characteristics in three devices demonstrate

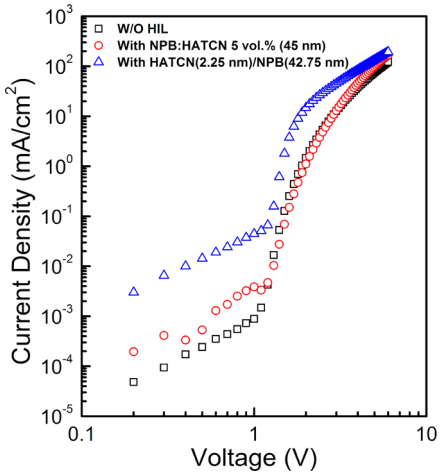


**Figure 5.** *J*−*V* characteristics of different HIL-based devices in double-logarithmic plots.

a typical trend from ohmic to trap-limited to trap-free SCL transport.[37] In general, the current at low bias is determined by the practical contact between the electrode and adjacent injection layer. As shown in Figure 5, the NPB:HATCN 5 vol. % (45 nm)-based device demonstrated a little higher current density than the device without any HILs in the low voltage


DOI: 10.1021/acsami.5b01989
ACS Appl. Mater. Interfaces 2015, 7, 11965−11971

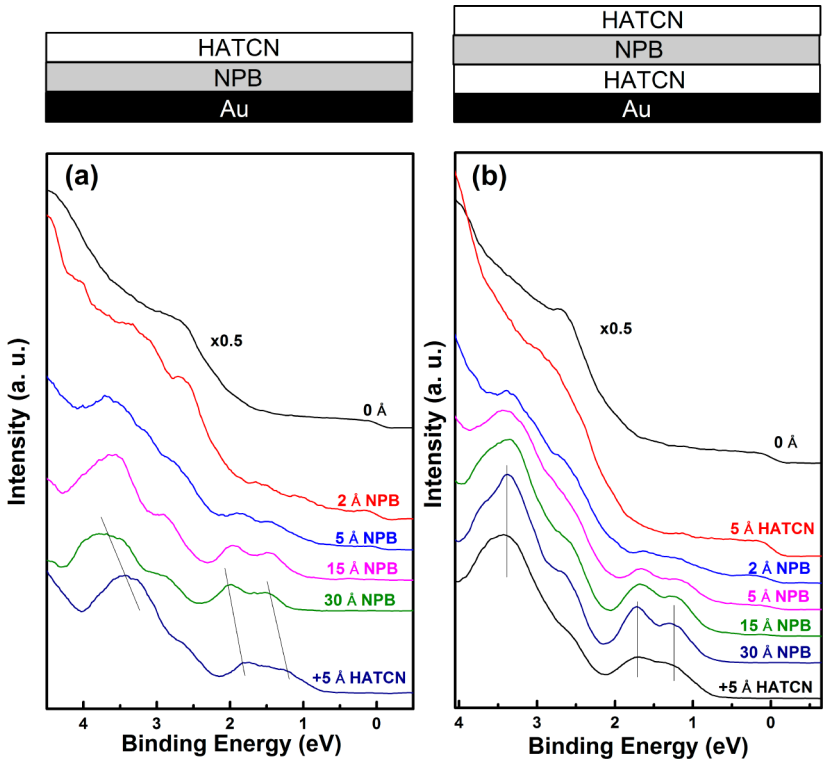


**Figure 6.** Thickness-dependent UPS spectra of NPB on (a) gold and (b) 5 Å HATCN/gold, in each case with a 5-Å-thick HATCN top layer.

range. Noticeably, in the whole voltage range, the pure HATCN (2.25 nm)-based device exhibited very obvious hole-injection enhancement compared to the NPB:HATCN 5 vol. % (45 nm)-based device. These results suggest a clear indication of the anode modification effect using HATCN as an HIL. In a word, the slightly improved performance in NPB:HATCN 5 vol. % (45 nm)-based OLEDs could be attributed to the ITO modification by the diffused HATCN molecules, which originated from the NPB:HATCN layer. A similar phenomenon has been reported in Duhm et al.'s work.[46,47] These results correspond with the performance of the device without the p-type effect in the NPB:HATCN film in Figure 1. A poorer OLED performance is obtained by using the HATCN-doped layer as the HIL because the doped HATCN decreases the conductivity in NPB, while the hole-injection ability is also worse than that of pristine HATCN.

Furthermore, the interfacial diffusion effect of the HATCN molecules was verified by the in situ UPS measurement. Figure 6 shows the thickness-dependent UPS spectra of NPB on gold (a) and on 5 Å HATCN/gold (b). In both cases, a 5-Å-thick HATCN top layer is deposited. The deposition sequence is sketched in the upper part of the figure. The shifts of the molecular features caused by the HATCN top layer are marked by lines. As shown in Figure 6a, the photoemission features of gold was attenuated by the deposition of NPB. The metal Fermi edge was totally suppressed in the case of a coverage of 15 Å NPB. It suggests that the entire gold substrate was covered with NPB completely. There should be no pinholes in the amorphous NPB film with a 30-Å-thick coverage. Noticeably, the deposition of a 5-Å-thick HATCN top layer on the thick NPB layer caused very rigid shifts in the BE. The shifts were assumed to relate to the HATCN diffusion through the NPB layer toward the gold substrate. The diffused HATCN then reacts with gold to form additional dipoles at the interface between the gold substrate and NPB layer. The generated dipoles shift the HOMO level of the material toward the Fermi energy ($E_F$) by 0.45 eV, which could be accurately seen from the change of the HIB (from 1.15 to 0.70 eV). For comparison, 5 Å HATCN was deposited first to modify the gold substrate, as shown in Figure 6b. With increasing thickness of NPB, the HIB varied from 0.76 to 0.79 eV. Subsequent deposition of a 5 Å HATCN layer on top of the NPB multilayer did not result in any significant changes in the UPS spectrum compared with that in Figure 6a. In all, HATCN can diffuse through 3 nm NPB to modify the gold electrode. The energy-level realignment was really observed by a top deposition of HATCN because of its diffusion toward the metal substrate and subsequent dipole layer formation. This gives a clue that the slightly improved device performance in NPB:HATCN-based OLEDs is mainly attributed to an interfacial modification effect owing to the interfacial diffusion of HATCN small molecules.

## 4. CONCLUSION

In summary, we have investigated the injection properties as well as the "doping" behavior of a strong electron acceptor, HATCN, in a typical hole-transport material, NPB. A slightly improved OLED performance was achieved by using HATCN-doped NPB as an HIL, whereas the hole-injection enhancement is inferior to the case of using pure HATCN as the HIL. Fundamental physical characteristics evaluations involving UV−vis and FTIR absorption and XPS revealed that there was no charge-transfer effect in the NPB:HATCN composite films. The current−voltage injection characteristics suggested that the improved performance in NPB:HATCN-based OLEDs was attributed to an interfacial modification effect owing to the interfacial diffusion of HATCN small molecules, which could be verified by the in situ UPS evaluations.


DOI: 10.1021/acsami.5b01989
ACS Appl. Mater. Interfaces 2015, 7, 11965−11971

## ■ ASSOCIATED CONTENT

### Supporting Information

Device performance of DCJTB-based OLEDs with NPB:HATCN and NPB:$MoO_3$ HILs and pristine HATCN (or $MoO_3$) HIL, $J-V$ characteristics of different hole-dominated devices, UPS measurement of different HILs with various HATCN doping ratios, PL spectra of NPB films with and without HATCN doping. The Supporting Information is available free of charge on the ACS Publications website at DOI: 10.1021/acsami.5b01989.

## ■ AUTHOR INFORMATION


### Corresponding Authors

*E-mail: zkwang@suda.edu.cn.
*E-mail: lsliao@suda.edu.cn.


### Notes

The authors declare no competing financial interest.

## ■ ACKNOWLEDGMENTS

We acknowledge financial support from the Natural Science Foundation of China (Grants 61177016 and 61307036), from the Natural Science Foundation of Jiangsu Province (Grant BK20130288), and from the Key University Science Research Project of Jiangsu Province (Grant SZ21407812). This project is also funded by the Priority Academic Program Development of Jiangsu Higher Education Institutions and by the Program for Graduate Research and Innovation in the Universities of Jiangsu Province (Grant CXLX13-795).

## ■ REFERENCES


(1) D'Andrade, B. W.; Forrest, S. R. White Organic Light-Emitting Devices for Solid-State Lighting. *Adv. Mater.* **2004**, *16*, 1585−1595.

(2) Ding, L.; Tang, X.; Xu, M. F.; Shi, X. B.; Wang, Z. K.; Liao, L. S. Lithium Hydride Doped Intermediate Connector for High-Efficiency and Long-Term Stable Tandem Organic Light-Emitting Diodes. *ACS Appl. Mater. Interfaces* **2014**, *6*, 18228−18232.

(3) Helander, M. G.; Wang, Z. B.; Qiu, J.; Greiner, M. T.; Puzzo, D. P.; Liu, Z. W.; Lu, Z. H. Chlorinated Indium Tin Oxide Electrodes with High Work Function for Organic Device Compatibility. *Science* **2011**, *332*, 944−947.

(4) Wang, Z.; Lou, Y.; Naka, S.; Okada, H. Bias and Temperature Dependent Charge Transport in Solution-Processed Small Molecular Mixed Single Layer Organic Light Emitting Devices. *Appl. Phys. Lett.* **2011**, *98*, 063302−063302.

(5) Gao, C. H.; Zhu, X. Z.; Zhang, L.; Zhou, D. Y.; Wang, Z. K.; Liao, L. S. Comparative Studies on the Inorganic and Organic p-Type Dopants in Organic Light-Emitting Diodes with Enhanced Hole Injection. *Appl. Phys. Lett.* **2013**, *102*, 153301.

(6) Wang, Z.; Lou, Y.; Naka, S.; Okada, H. Temperature Dependence of Carrier Injection in Small Molecular Organic Light Emitting Device with a Mixed Single Layer. *Chem. Phys. Lett.* **2010**, *501*, 75−79.

(7) Lee, H.; Cho, S. W.; Han, K.; Jeon, P. E.; Whang, C. N.; Jeong, K.; Cho, k.; Yi, Y. The Origin of the Hole Injection Improvements at Indium Tin Oxide/Molybdenum Trioxide/*N*,*N*′-Bis(1-Naphthyl)-*N*,*N*′-Diphenyl-1,1′-Biphenyl- 4,4′-Diamine Interfaces. *Appl. Phys. Lett.* **2008**, *93*, 043308.

(8) Gao, C. H.; Cai, S. D.; Gu, W.; Zhou, D. Y.; Wang, Z. K.; Liao, L. S. Enhanced Hole Injection in Phosphorescent Organic Light-Emitting Diodes by Thermally Evaporating a Thin Indium Trichloride Layer. *ACS Appl. Mater. Interfaces* **2012**, *4*, 5211−5216.

(9) Koch, N.; Duhm, S.; Rabe, J. P.; Vollmer, A.; Johnson, R. L. Optimized Hole Injection with Strong Electron Acceptors at Organic−Metal Interfaces. *Phys. Rev. Lett.* **2005**, *95*, 237601.

(10) Hanson, E. L.; Guo, J.; Koch, N.; Schwartz, J.; Bernasek, S. L. Advanced Surface Modification of Indium Tin Oxide for Improved Charge Injection in Organic Devices. *J. Am. Chem. Soc.* **2005**, *127*, 10058−10062.

(11) McDowell, M.; Hill, I. G.; McDermott, J. E.; Bernasek, S. L.; Schwartz, J. Improved Organic Thin-Film Transistor Performance Using Novel Self-Assembled Monolayers. *Appl. Phys. Lett.* **2006**, *88*, 073505.

(12) Shi, X. B.; Xu, M. F.; Zhou, D. Y.; Wang, Z. K.; Liao, L. S. Improved Cation Valence State in Molybdenum Oxides by Ultraviolet-Ozone Treatments and its Applications in Organic Light-Emitting Diodes. *Appl. Phys. Lett.* **2013**, *102*, 233304.

(13) Liang, J.; Zu, F. S.; Ding, L.; Xu, M. F.; Shi, X. B.; Wang, Z. K.; Liao, L. S. Aqueous Solution-Processed $MoO_3$ Thick Films as Hole Injection and Short-Circuit Barrier Layer in Large-Area Organic Light-Emitting Devices. *Appl. Phys. Exp.* **2014**, *7*, 111601.

(14) Lee, J. H.; Leem, D. S.; Kim, H. J.; Kim, J. J. Effectiveness of p-Dopants in an Organic Hole Transporting Material. *Appl. Phys. Lett.* **2009**, *94*, 123306.

(15) Leem, D. S.; Park, H. D.; Kang, J. W.; Lee, J. H.; Kim, J. W.; Kim, J. J. Low Driving Voltage and High Stability Organic Light-Emitting Diodes with Rhenium Oxide-Doped Hole Transporting Layer. *Appl. Phys. Lett.* **2007**, *91*, 011113.

(16) Lou, Y. H.; Xu, M. F.; Zhang, L.; Wang, Z. K.; Naka, S.; Okada, H.; Liao, L. S. Origin of Enhanced Electrical and Conducting Properties in Pentacene Films Doped by Molybdenum Trioxide. *Org. Electron.* **2013**, *14*, 2698−2704.

(17) Lou, Y. H.; Xu, M. F.; Wang, Z. K.; Naka, S.; Okada, H.; Liao, L. S. Dual Roles of $MoO_3$-Doped Pentacene Thin Films as Hole-Extraction and Multicharge-Separation Functions in Pentacene/$C_{60}$ Heterojunction Organic Solar Cells. *Appl. Phys. Lett.* **2013**, *102*, 113305.

(18) Blochwitz, J.; Pfeiffer, M.; Fritz, T.; Leo, K. Low Voltage Organic Light Emitting Diodes Featuring Doped Phthalocyanine as Hole Transport Material. *Appl. Phys. Lett.* **1998**, *73*, 729.

(19) Zhou, X.; Blochwitz, J.; Pfeiffer, M.; Nollau, A.; Fritz, T.; Leo, K. Enhanced Hole Injection into Amorphous Hole-Transport Layers of Organic Light-Emitting Diodes Using Controlled p-Type Doping. *Adv. Funct. Mater.* **2001**, *11*, 310−314.

(20) Zhou, X.; Pfeiffer, M.; Blochwitz, J.; Werner, A.; Nollau, A.; Fritz, T.; Leo, K. Very-Low-Operating-Voltage Organic Light-Emitting Diodes Using a p-Doped Amorphous Hole Injection Layer. *Appl. Phys. Lett.* **2001**, *78*, 410.

(21) Ding, L.; Sun, Y. Q.; Chen, H.; Zu, F. S.; Wang, Z. K.; Liao, L. S. A Novel Intermediate Connector with Improved Charge Generation and Separation for Large-Area Tandem White Organic Lighting Devices. *J. Mater. Chem. C* **2014**, *2*, 10403−10408.

(22) Kanno, H.; Holmes, R. J.; Sun, Y.; Kena-Cohen, S.; Forrest, S. R. White Stacked Electrophosphorescent Organic Light-Emitting Devices Employing $MoO_3$ as a Charge-Generation Layer. *Adv. Mater.* **2006**, *18*, 339−342.

(23) Niederhausen, J.; Amsalem, P.; Frisch, J.; Wilke, A.; Vollmer, A.; Rieger, R.; Müllen, K.; Rabe, J. P.; Koch, N. Tuning Hole-Injection Barriers at Organic/Metal Interfaces Exploiting the Orientation of a Molecular Acceptor Interlayer. *Phys. Rev. B* **2011**, *84*, 165302.

(24) Jang, S. E.; Lee, J. Y. Organic Interlayer for High Power Efficiency in Organic Light-Emitting Diodes. *Synth. Met.* **2011**, *161*, 40−43.

(25) Jeon, W. S.; Park, J. S.; Li, L.; Lim, D. C.; Son, Y. H.; Suh, M. C.; Kwon, J. H. High Current Conduction with High Mobility by Non-Radiative Charge Recombination Interfaces in Organic Semiconductor Devices. *Org. Electron.* **2012**, *13*, 939−944.

(26) Park, S. M.; Kim, Y. H.; Yi, Y.; Oh, H. Y.; Kim, J. W. Insertion of an Organic Interlayer for Hole Current Enhancement in Inverted Organic Light Emitting Devices. *Appl. Phys. Lett.* **2010**, *97*, 063308.

(27) Kim, Y. K.; Kim, J. W.; Park, Y. Energy Level Alignment at a Charge Generation Interface between 4,4′-Bis(*N*-phenyl-1-naphthylamino)biphenyl and 1,4,5,8,9,11-Hexaazatriphenylene-Hexacarbonitrile. *Appl. Phys. Lett.* **2009**, *94*, 063305.




DOI: 10.1021/acsami.5b01989
*ACS Appl. Mater. Interfaces* 2015, 7, 11965−11971

(28) Yook, K. S.; Jeon, S. O.; Lee, J. Y. Efficient Hole Injection by Doping of Hexaazatriphenylene Hexacarbonitrile in Hole Transport Layer. *Thin Solid Films* **2009**, *517*, 6109−6111.
(29) Small, C. E.; Tsang, S. W.; Kido, J.; So, S. K.; So, F. Origin of Enhanced Hole Injection in Inverted Organic Devices with Electron Accepting Interlayer. *Adv. Mater.* **2012**, *22*, 3261−3266.
(30) Noguchi, Y.; Lim, H.; Isoshima, T.; Ito, E.; Hara, M.; Chin, W. W.; Han, J. W.; Kinjo, H.; Ozawa, Y.; Nakayama, Y.; Ishii, H. Influence of The Direction of Spontaneous Orientation Polarization on the Charge Injection Properties of Organic Light-Emitting Diodes. *Appl. Phys. Lett.* **2013**, *102*, 203306.
(31) Perumal, A.; Lüssem, B.; Leo, K. High Brightness Alternating Current Electroluminescence with Organic Light Emitting Material. *Appl. Phys. Lett.* **2012**, *100*, 103307.
(32) Park, Y. W.; Choi, J. H.; Park, T. H.; Song, E. H.; Kim, H.; Lee, H. J.; Shin, S. J.; Ju, B. K.; Song, W. J. Role of n-Dopant Based Electron Injection Layer in n-Doped Organic Light-Emitting Diodes and its Simple Alternative. *Appl. Phys. Lett.* **2012**, *100*, 013312.
(33) Lou, Y.; Okawa, Y.; Wang, Z.; Naka, S.; Okada, H. Efficient Electron Transport in 4,4′-Bis[*N*-(1-Napthyl)-*N*-Phenyl-Amino]-biphenyl and the Applications in White Organic Light Emitting Devices. *Org. Electron.* **2013**, *14*, 1015−1020.
(34) Cho, S. H.; Pyo, S. W.; Suh, M. C. Low Voltage Top-Emitting Organic Light Emitting Devices By Using 1,4,5,8,9,11-Hexaazatriphenylene-Hexacarbonitrile. *Synth. Met.* **2012**, *162*, 402−405.
(35) Yook, K. S.; Jeon, S. O.; Joo, C. W.; Lee, J. Y. Hole Injection Improvement by Doping of Organic Material in Copper Phthalocyanine. *J. Ind. Eng. Chem.* **2009**, *15*, 907−909.
(36) Lee, J. H.; Kim, H. M.; Kim, K. B.; Kabe, R.; Anzenbacher, P.; Kim, J. J. Homogeneous Dispersion of Organic p-Dopants in an Organic Semiconductor as an Origin of High Charge Generation Efficiency. *Appl. Phys. Lett.* **2011**, *98*, 173303.
(37) Qi, Y.; Sajoto, T.; Barlow, S.; Kim, E. G.; Brédas, J. L.; Marder, S. R.; Kahn, A. Use of a High Electron-Affinity Molybdenum Dithiolene Complex to p-Dope Hole-Transport Layers. *J. Am. Chem. Soc.* **2009**, *131*, 12530−12531.
(38) Small, C. E.; Tsang, S. W.; Kido, J.; So, S. K.; So, F. Origin of Enhanced Hole Injection in Inverted Organic Devices with Electron Accepting Interlayer. *Adv. Funct. Mater.* **2012**, *22*, 3261−3266.
(39) Wu, S. P.; Kang, Y.; Liu, T. L.; Jin, Z. H.; Jiang, N.; Lu, Z. H. Formation of Charge-Transfer Complex in Organic:Metal Oxides Systems. *Appl. Phys. Lett.* **2013**, *102*, 163304.
(40) Qiao, X.; Chen, J.; Li, X.; Ma, D. Observation of Hole Hopping via Dopant in $MoO_x$-Doped Organic Semiconductors: Mechanism Analysis and Application for High Performance Organic Light-Emitting Devices. *J. Appl. Phys.* **2010**, *107*, 104505.
(41) Ho, C. L.; Wong, W. Y.; Wang, Q.; Ma, D.; Wang, L.; Lin, Z. A Multifunctional Iridium-Carbazolyl Orange Phosphor for High-Performance Two-Element WOLED Exploiting Exciton-Managed Fluorescence/Phosphorescence. *Adv. Funct. Mater.* **2008**, *18*, 928−937.
(42) Vasilopoulou, M.; Douvas, A. M.; Georgiadou, D. G.; Palilis, L. C.; Kennou, S.; Sygellou, L.; Argitis, P. The Influence of Hydrogenation and Oxygen Vacancies on Molybdenum Oxides Work Function and Gap States for Application in Organic Optoelectronics. *J. Am. Chem. Soc.* **2012**, *134*, 16178−16187.
(43) Greiner, M. T.; Helander, M. G.; Wang, Z. B.; Tang, W. M.; Qiu, J.; Lu, Z. H. A Metallic Molybdenum Suboxide Buffer Layer for Organic Electronic Devices. *Appl. Phys. Lett.* **2010**, *96*, 213302.
(44) Meyer, J.; Hamwi, S.; Kröger, M.; Kowalsky, W.; Riedl, T.; Kahn, A. Transition Metal Oxides for Organic Electronics: Energetics, Device Physics and Applications. *Adv. Mater.* **2012**, *24*, 5408−5427.
(45) Zhuang, T.; Wang, X. F.; Sano, T.; Hong, Z.; Li, G.; Yang, Y.; Kido, J. Fullerene C70 as a P-type Donor in Organic Photovoltaic Cells. *Appl. Phys. Lett.* **2014**, *10*, 093301.
(46) Duhm, S.; Salzmann, I.; Bröker, B.; Glowatzki, H.; Johnson, R. L.; Koch, N. Interdiffusion of Molecular Acceptors through Organic Layers to Metal Substrates Mimics Doping-Related Energy Level Shifts. *Appl. Phys. Lett.* **2009**, *95*, 093305.
(47) Amsalem, P.; Wilke, A.; Frisch, J.; Niederhausen, J.; Vollmer, A.; Rieger, R.; Koch, N. Interlayer Molecular Diffusion and Thermodynamic Equilibrium in Organic Heterostructures on a Metal Electrode. *J. Appl. Phys.* **2011**, *110*, 113709.


DOI: 10.1021/acsami.5b01989
*ACS Appl. Mater. Interfaces* 2015, 7, 11965−11971